proposed in this paper) by a significant amount (but see the example due to Hendrickson et al.,[27] which proposes just such an exception). Thus, the proposal of a limit function to long-range superexchange presents a clear challenge to experimentalists, which is to produce one or more exceptions to the limit curve we propose, and to the theorists to explain why!

Supplementary Material Available: Appendix I and an additional list of references pertinent to Figures 1 and 2 (7 pages). Ordering information is available on any current masthead page.

References and Notes

(1) M. Nakayama, *J. Phys. Soc. Jpn.*, **40**, 82–89 (1976).
(2) R. L. Martin, "Metal-Metal Interactions in Paramagnetic Clusters", in "New Pathways in Inorganic Chemistry", E. A. V. Ebsworth, A. G. Maddock, and A. G. Sharpe, Ed., Cambridge University Press, London, 1968.
(3) V. H. Crawford, H. W. Richardson, J. R. Wasson, D. J. Hodgson, and W. E. Hatfield, *Inorg. Chem.*, **15**, 2107–2110 (1976).
(4) J. B. Goodenough, *Phys. Chem. Solids*, **6**, 287 (1958).
(5) J. Kanamori, *Phys. Chem. Solids*, **10**, 87 (1959).
(6) D. Bloch, *J. Phys. Chem. Solids*, **27**, 881–885 (1966).
(7) E. A. Harris, *J. Phys. C: Solid State Phys.*, **5**, 338–352 (1972).
(8) K. N. Shrivastava and V. Jaccarino, *Phys. Rev.*, **13**, 299 (1976).
(9) K. C. Johnson and A. J. Sievers, *Phys. Rev. B*, **10**, 1027–1038 (1974).
(10) M. T. Hutchings, R. J. Birgeneau, and W. P. Wolf, *Phys. Rev.*, **168**, 1026–1044 (1968).
(11) F. Keffer and T. Oguchi, *Phys. Rev.*, **115**, 1428 (1959).
(12) N. H. L. Liu and R. Orbach, *AIP Conf. Proc.*, *1972*, **No. 10**, part 2, 1238–1255 (1973).
(13) R. D. Harcourt and G. E. Martin, *J. Chem. Soc., Faraday Trans. 2*, 1–14 (1977).
(14) I. B. Bersuker and Yu. G. Titova, *Theor. Expt. Chem.*, **6**, 381 (1970).
(15) P. W. Anderson, *Phys. Rev.*, **115**, 2 (1959).
(16) Y. Sugiura, *Z. Phys.*, **45**, 484–492 (1927).
(17) C. Herring and M. Flicker, *Phys. Rev. A*, **134**, 362 (1964).
(18) C. Herring, "Direct Exchange between Well-Separated Atoms", in "Magnetism", Vol. IIB, G. T. Rado and H. Suhl, Ed., 1966, pp 1–181.
(19) E. A. Mason and L. Monchick, *Adv. Chem. Phys.*, **12**, 338–343 (1967).
(20) H. O. Knox and M. R. H. Rudge, *Mol. Phys.*, No. 4, 377–380 (1969).
(21) Y.-H. Uang and W. C. Stwalley, to be published.
(22) M. L. Olson and D. D. Konowalow, *Chem. Phys.*, **21**, 393 (1977).
(23) W. Geertsma, C. Haas, G. A. Sawatzky, and G. Vertogen, *Physica*, **86–88B**, 1039–1040 (1977).
(24) M. A. Ruderman and C. Kittel, *Phys. Rev.*, **96**, 99 (1954); T. Kasuya, *Prog. Theor. Phys. (Kyoto)*, **16**, 45 (1956); K. Yosida, *Phys. Rev.*, **106**, 893 (1957).
(25) J. Kondo, *Solid State Phys.*, **23**, 183–281 (1969).
(26) A. Yu, Kozhuhar and G. A. Tsintsadze, *Phys. Lett. A*, **55**, 175–176 (1975).
(27) T. R. Felthouse and D. N. Hendrickson, *Inorg. Chem.*, **17**, 2636 (1978).
(28) R. Plumier and F. K. Lotgering, *Solid State Commun.*, **8**, 477–480 (1970).
(29) P. W. Anderson, *Phys. Rev.*, **79**, 705 (1950).
(30) J. B. Torrance, F. Holtzberg, and T. R. McGuire, *AIP Conf. Proc.*, **No. 10**, 1279 (1973).

General Magnetic Dipolar Interaction of Spin–Spin Coupled Molecular Dimers. Application to an EPR Spectrum of Xanthine Oxidase

R. E. Coffman* and G. R. Buettner†

Department of Chemistry, The University of Iowa, Iowa City, Iowa 52242 (Received April 20, 1979)

An analysis is given of the general spin–spin dipolar interaction in the presence of a general bilinear superexchange interaction, and its effects on a rigid lattice EPR line shape are calculated. The general magic angle effect is considered, numerically, for specific cases of both single crystal spectra and randomly oriented microcrystallite samples. Analysis of the number of determinable spin–spin coupling coefficients suggests that a component analysis can be developed which can yield useful information about the geometrical arrangement of two interacting spin = $1/2$ molecules, as well as covalency information about the interaction. This analysis is applied to a Mo(V)–iron sulfur interaction in xanthine oxidase and xanthine dehydrogenase, which has been described by Lowe and Bray. Line shape calculations show that the observed small amount of dipolar anisotropy is consistent with a separation of the Mo(V) and Fe/S groups of 14 Å or less. Considerations of the long-range nature of superexchange, from existing experimental data on superexchange, are consistent with this estimate.

I. Introduction

Several recent EPR studies of paramagnetic metal-metal and metal-free radical interactions in metalloenzymes and model complexes have concerned systems where the apparent distance of the dipolar and exchange interactions is decidedly long range, i.e., 8–10 Å or longer. Since exchange interactions decrease exponentially vs. R and dipolar interactions decrease as $1/R^3$, it is evident that dipolar anisotropy must be a prominent feature of long-range spin–spin coupling. It should therefore be possible to extract useful structural information from spin–spin interactions in EPR spectra of this type. It is also possible to obtain information about the exchange tensor, par-

ticularly the sign and magnitude of the scalar component of the exchange interaction. The vector and tensor components of the exchange interaction are frequently much smaller than the scalar component which then simplifies the form of the interaction. The dipolar "magic angle" effect may also play a prominent role in the spectrum, particularly for random orientation samples, since this effect may lead to a vanishing of the dipolar splitting at one or more "turning-points" of the spectrum. The relatively narrow EPR line widths (of solid samples) which may be expected as a result of both increased magnetic dilution and a magic-angle collapse of the dipolar splitting (and the existence of systems displaying these effects) provide a means for investigating the nature of long-range exchange interactions. For these reasons,

† Wabash College, Crawfordsville, Ind. 47933.

© 1979 American Chemical Society

among others, we have studied the general dipole–dipole and exchange interactions when both operators are present and of comparable magnitude.

The phenomenological operator physics necessary to describe the combined effects of both exchange (EX) and magnetic dipole–dipole (DD) interactions is, in principle, well known. It has not previously been developed and used in full generality, however, a fact reflected by the frequent incorrect use of magnetic dipole–dipole formulae for EPR distance estimation. In addition, certain logical problems arise when both exchange and dipolar effects are of comparable magnitude, and one tries to separate them into unique components by computational means. This is precisely the problem which arose in our attempts to determine the "magnetic geometry" of a coenzyme B_{12}–free-radical complex from a rigid lattice EPR spectrum.[1] The distance between centers of unpaired spin density in this example appeared to be relatively large (ca. 10 Å). A general study of the latter problem requires the study of two separate effects: the magic angle effect, and the nature of the limits to long-range superexchange interaction.

The purpose of this paper, then, is to present a general analysis of the various spin–spin interactions in a form which delineates the state of present understanding of the phenomenological operator physics of these effects, and points the way toward future theoretical and experimental work. This study is particularly oriented toward the analysis of long-range spin–spin coupling effects in metalloenzymes since these systems are generally magnetically dilute and represent examples of magnetic interactions not commonly found in smaller molecules.

The plan of the paper is as follows: the major topics appear under the headings: I. Introduction, II. Historical Resume, III. General Point Dipole–Point Dipole Magnetic Interaction, IV. General Magic Angle Effect, V. Combined Dipolar Plus Bilinear Exchange Interaction, VI. Mo(V)–Iron/Sulfur Long-Range Spin–Spin Interaction in Xanthine Oxidase and Xanthine Dehydrogenase, and VII. Conclusions.

II. Historical Resume

The EPR line shape arising as a result of bilinear spin–spin interaction is a function of several physical properties which a comprehensive theory must correctly represent. These are (i) the effects of magnetic anisotropies present in interacting spin systems, (ii) the effect of the relative orientations of one spin system relative to the other, (iii) the effect of delocalized spin density on the magnetic dipolar interaction, and (iv) the effects of the different lifetimes of the components of the spin polarizations. We will here consider some aspects of (i) and (ii), but inclusion of (iii) and (iv) will necessitate a more general formulation of the physics (quantum and statistical density matrices) than is warranted to use here.

One of the first detailed analyses of a dipolar spin–spin interaction was that of Pake[2] who determined the relative direction of the interproton vector in $CaSO_4 \cdot 2H_2O$ by a study of proton magnetic resonance fine structure. A recent development for EPR distance measurement is the treatment due to Leigh[3] of the dipolar interaction between two rigidly fixed spins where the lifetime of one spin is much shorter than the other. More recent treatments are those of Chao[4] who applied the Wigner–Eckart theorem in deriving a spin Hamiltonian for strongly exchange and dipolar coupled spin–spin pairs, and two papers from Pilbrow's group which treat, in detail and with considerable generality, the perturbation theory appropriate to both strongly and weakly coupled pairs of Cu(II) ions. The latter two papers, by Carr et al.[5] and Boyd et al.,[6] are

interesting in that they establish a strong correspondence (in these cases) between the "magnetic geometry", established from analysis of the dipolar angular orientations, and the true crystallographic geometry. The most recent treatment of the perturbation theory of the bilinear spin–spin interaction in EPR and application to some coenzyme B_{12} problems is that of Boas, Hicks, Pilbrow, and Smith,[7] to which the reader is referred for the complete details of a perturbation theory treatment of some aspects of the problem treated here.

The present authors have recently used[1] an indirect, exact numerical method to determine the Co(II)–free-radical magnetic geometry in a paramagnetic coenzyme B_{12}–enzyme system in which the spin–spin coupling is due to a small scalar exchange coupling with a dipolar spin-spin coupling of comparable magnitude. In an earlier study by Schepler et al.[8] of a series of systems of this type (the "doublet" spectrum) it had been proposed that the apparent vanishing of dipolar effects in the spectrum was due to a special "magic angle" geometry which existed uniformly in a series of systems in which there was considerable variation of the **g** tensors. Further analysis showed this hypothesis to be wrong, but it did raise the question of how the "magic angle" depends on the anisotropies of the two **g** tensors, and over what range of geometries a collapsed dipolar splitting might be observed.

Another stimulus to this study of long-range spin–spin coupling is the problem of the clearly very small dipolar anisotropy in the EPR spectra of interacting Mo(V) and Fe/S groups (both $S = 1/2$) in xanthine oxidase and xanthine dehydrogenase. These studies, by Lowe and Bray,[9] are directed toward the discovery of the geometric arrangement of the two paramagnetic groups and the pathway of interaction through the macromolecule. However, as they point out, the problem of selecting the mechanism responsible for the very small dipolar anisotropy presents a trilemma: it could be due to the magic angle effect (a very special situation), it could be due to an isotropic spin–spin interaction acting over a *very* long range, or it could be due to a third, undiscovered mechanism. One of the goals of this study, in relation to this particular problem, is to determine whether a combination of the first two alternative solutions might be a satisfactory solution to Lowe and Bray's problem. In order to do this, we need a reasonably complete description of the general spin–spin coupling effect, suitable to a rigid lattice EPR problem.

III. General Point Dipole–Point Dipole Magnetic Interaction

The spin Hamiltonian for the dipole–dipole interaction between two electronic magnetic moments with isotropic g values g_1 and g_2 is well approximated by

$$\mathcal{H} = \beta g_1 \vec{B} \cdot \vec{S}_1 + \beta g_2 \vec{B} \cdot \vec{S}_2 + \frac{g_1 g_2 \beta^2}{R_{12}{}^3}(1 - 3\cos^2 \zeta) S_{1Z} S_{2Z} \quad (1)$$

where ζ is the angle between the magnetic field direction (here, the axis of quantization) and the vector from the center of spin density of molecule 1 to the corresponding center for molecule 2. The dipolar splitting vanishes when the angle ζ satisfies the condition $1 - 3\cos^2 \zeta = 0$, for which $\zeta_{magic} = 54° \ 44' = 54.736°$. If there is **g** tensor anisotropy for either one or both spins, then the dipolar interaction depends on two spherical angles: ζ and η (see Figure 1). The additional **g** tensor parameters and the various rotational angles can only be included in general dipolar effect considerations by using a form of $\mathcal{H}_{dd}$ which is a complete (rather than truncated) form of the dipolar
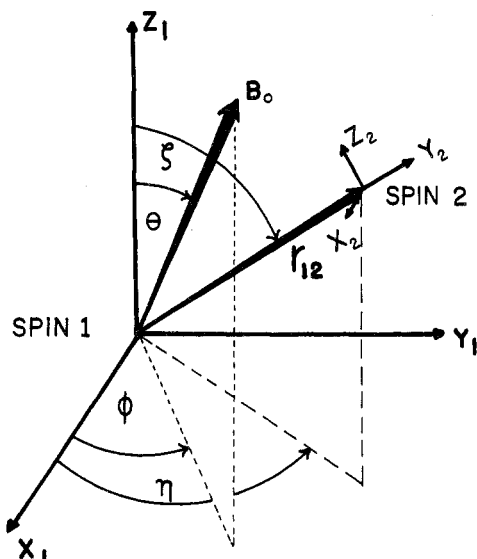
Figure 1. The spherical coordinate system used to describe the orientation of spin system 2 with respect to the principal axis system of spin system 1. The orientation of the magnetic field is given by the angles θ and φ; the orientation of the vector from spin 1 to spin 2 is given by ζ, η, and the Eulerian angles α, β, and γ determine the orientation of coordinate system 2 relative to the principal axis system of spin 1.

operator. For this reason, it is more convenient to use a fixed quantization scheme, since a direct numerical approach will be used to calculate dipolar fine structure.

The general spin Hamiltonian for two interacting $S = 1/2$ spin systems may be written as $\mathcal{H} = \mathcal{H}_1 + \mathcal{H}_2 + \mathcal{H}_{12}$, where $\mathcal{H}_1$ and $\mathcal{H}_2$ contain the electronic and nuclear Zeeman operators as well as the nuclear hyperfine and quadrupole moment operators. $\mathcal{H}_{12}$ contains the general exchange and magnetic dipole–dipole interactions. In this section, we shall restrict the independent operators $\mathcal{H}_1$ and $\mathcal{H}_2$ to be strictly Zeeman in character, and $\mathcal{H}_{12}$ is to be purely dipolar:

$$\mathcal{H} = \beta \vec{B}^t \cdot \mathbf{g}_1 \cdot \vec{S}_1 + \beta \vec{B}^t \cdot \mathbf{g}_2 \cdot \vec{S}_2 + \mathcal{H}_{dd} \tag{2}$$

The classical magnetic dipole interaction energy has the form

$$W_{dd} = \frac{\vec{\mu}_1 \cdot \vec{\mu}_2}{R_{12}^3} - \frac{3(\vec{\mu}_1 \cdot \hat{r})(\vec{\mu}_2 \cdot \hat{r})}{R_{12}^3} \tag{3}$$

The corresponding quantum mechanical operator is obtained by making the substitutions $\vec{\mu} = -\beta \mathbf{g}_1 \mathbf{S}_1$ and $\vec{\mu}_2 = -\beta \mathbf{g}_2 \mathbf{S}_2$. Here, $\mathbf{g}_1$ is the **g** matrix for spin 1, $\mathbf{S}_1$ is a column vector with components S_{1x}, S_{1y}, S_{1z}, and similarly for spin 2. The coordinate system, fixed with respect to spin 1, is chosen so that $\mathbf{g}_1$ is diagonal with components $g_{xx}^{(1)}$, $g_{yy}^{(1)}$, $g_{zz}^{(1)}$. The general location and orientation of spin 2, with respect to 1, is shown in Figure 1. In addition to the distance R_{12} and the spherical angles ζ and η, the coordinate system in which $\mathbf{g}_2$ is diagonal may be rotated (by nature, for the given pair of spins) through a set of Eulerian angles $-\alpha$, $-\beta$, $-\gamma$ from the reference coordinate system. Thus, in the reference frame of spin 1, the **g** tensor of spin 2 is generally not diagonal. Making these substitutions in eq 2, we find that the dipole–dipole energy operator assumes the form

$$\mathcal{H}_{dd} = \frac{\beta^2 (\mathbf{g}_1 \mathbf{S}_1)^t \mathbf{g}_2 \mathbf{S}_2}{R_{12}^3} - \frac{3\beta^2 \{(\mathbf{g}_1 \mathbf{S}_1)^t \mathbf{r}\}\{(\mathbf{g}_2 \mathbf{S}_2)^t \mathbf{r}\}}{R_{12}^3} \tag{4}$$

where t represents the matrix transpose operation, and **r** is a column vector of direction cosines (the elements of $\hat{r} = \vec{R}_{12}/|R_{12}|$).

Expansion of this operator into a useful form is a tedious process which needs only to be done once, if the expansion is sufficiently general. Since $\mathcal{H}_{dd}$ is bilinear in the spin operators, it may be expanded into the form

$$\hat{\mathcal{H}}_{dd} = \sum_{i,j=x,y,z} J_{ij}^{DD} \hat{S}_{1i} \hat{S}_{2j} \tag{5}$$

with nine dipole–dipole coefficient terms J_{xx}^{dd}, J_{xy}^{dd}, J_{xz}^{dd}, J_{yx}^{dd}, ..., J_{zz}^{dd}. Explicit expressions for these nine quantities, expressed in terms of the diagonal g values of each spin, and the six distance and angular variables R_{12}, ζ, η, α, β, and γ may be developed in a number of different ways. Pilbrow[6] has given a single general expansion formula entirely in terms of the diagonal **g** tensors and Eulerian angles. We give, in Appendix I (see paragraph at end of text regarding supplementary material), the nine dipole–dipole coefficients, J_{ij}^{dd}, expressed in terms of the diagonal **g** tensor of spin 1, and the generally nondiagonal **g** tensor of spin 2. The user of these expressions is therefore free to make his/her own choice of Eulerian angles and rotations. Matrix elements of $\mathcal{H}_{dd}$, using the J_{ij}^{DD}, are then easily found by using the expansion of $\mathcal{H}_{dd}$ into the convenient operator set $S_1^+ S_2^+$, ..., $S_{1z}S_{2z}$.

IV. General Magic Angle Effect

The magic angle effect is frequently invoked to explain the absence of dipolar splitting in EPR powder spectra of a two-spin system or to justify the neglect of the use of the dipolar operator in fitting a spectrum with an exchange coupling operator. We have therefore examined two separate but related properties: the dependence of the magic angle (defined as the angle causing collapse of the dipolar splitting) on **g** tensor anisotropy, and the relation between the true dipolar splitting and that obtained in a numerically synthesized powder spectrum.

For the case of isotropic **g** tensors the quantization reference frame may be arbitrarily rotated. For convenience, i.e., to diagonalize the dipolar coupling tensor, the z axis of the coordinate system is typically aligned with the interspin vector. This arrangement allows the dipole–dipole interaction to be represented by eq 1. The magic angle effect of eq 1 is the vanishing of the dipolar splitting when the angle between the interspin vector and the external magnetic field satisfies the condition $\zeta = 54.736°$. However, in a fixed quantization scheme (Figure 1) the magic angle effect may be observed when the magnetic field is along the x, y, or z axis.

When the **g** tensors of both spins are isotropic, the magic angle condition for B_0 along any principal axis is easily expressed with direction cosines. For $B_0 \parallel z$, the magic angle is $\zeta = \zeta_m = 54.736°$, and η_m = any value. The direction cosines of $\hat{r}$ are $\sin \zeta \cos \eta$ along the x axis, and $\sin \zeta \sin \eta$ along the y axis. Thus, for $B_0 \parallel x$ or y, the "magic" values ζ_m and η_m are determined by the solutions to

$$\sin \zeta_m \cos \eta_m = \cos (54.735°) \qquad B_0 \parallel x \tag{6a}$$

$$\sin \zeta_m \sin \eta_m = \cos (54.735°) \qquad B_0 \parallel y \tag{6b}$$

For the particular solution $\zeta_m = 54.736°$, $\eta_m = 45°$, the dipolar splitting vanishes for all measurements along the x, y, or z axes. Thus, this special angle pair is triply magic, and we refer to this pair of angles (54.736°, 45°) as the "trimagic" angle. Note that the trimagic angle direction is the same as the (111) direction in a simple cubic cell.

Another interesting feature is how ζ_m varies vs. η_m. Figures 2 and 3 show the variation observed in the dipolar splittings in the g_{zz} and g_{xx} regions of calculated spectra (g_{xx}, g_{yy}, and g_{zz} represent the principal values of the **g** tensors of the spin systems). In these model calculations
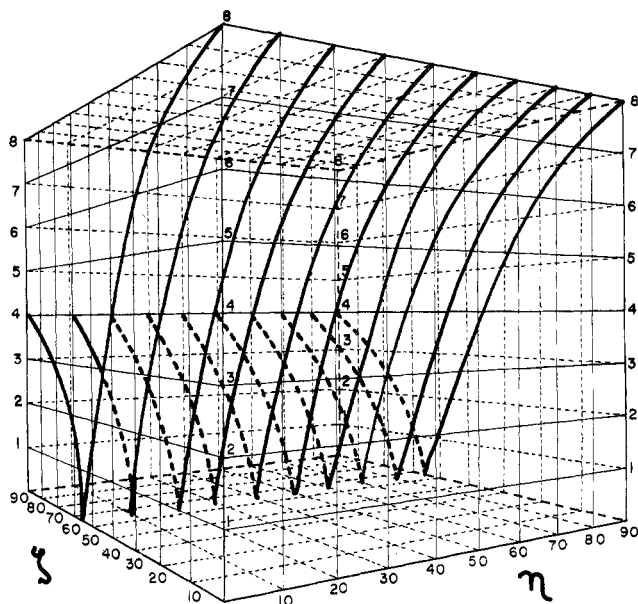
Figure 2. The ideal magic angle effect in the g_{zz} region of the spectrum. The value of the vertical axis times 10 represents the movement (in gauss) of the high-field g_{zz} line from where it would have occurred had no interaction been present. The dipolar separation is 7 Å. The principal axis systems of the two spins are parallel for all sets of orientation (ζ, η).
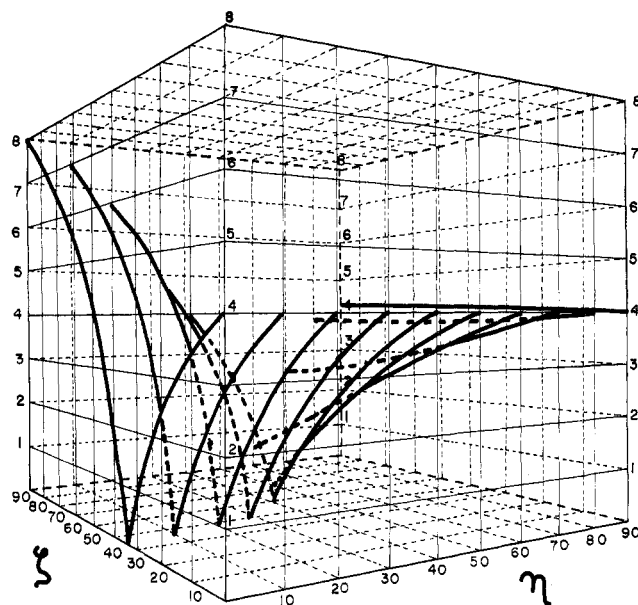
Figure 3. The ideal magic angle effect in the g_{xx} region. The splitting (in gauss) is the value of the vertical axis on the graph multiplied by 20. The dipolar separation is 7 Å. The principal axis systems of the two spins are parallel for all sets of orientation (ζ, η). The figure for the g_{yy} region may be obtained by reflecting the g_{xx} surface through a plane that is parallel with the vertical axis and that passes through the points ($\zeta = 0°$, $\eta = 0°$) and ($\zeta = 90°$, $\eta = 90°$).

the **g** tensors of the two spins were identical and the principal axis systems of the two **g** tensors were kept parallel as various spatial orientations were considered. The distance between the two dipoles was 7 Å. In Figure 2 the vertical axis shows the movement upfield of the high-field g_{zz} line (vertical axis value × 10 = gauss moved) from where it would have occurred had no interaction been present. The two horizontal axes are the ζ or η angles of Figure 1. In Figure 3 the vertical axis represents the splitting in the g_{xx} region of the spectra. The actual splitting, in gauss, is the value of the vertical axis on the graph multiplied by 20. Thus, in Figure 3 for the ori-
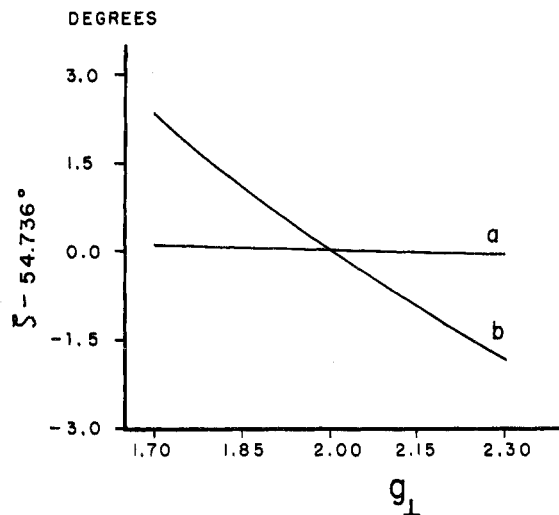
Figure 4. Two identical axially symmetric spin systems with their $g_{\parallel}$ axes collinear are used to demonstrate the deviation of the magic angle (i.e., the value of ζ for which the dipolar splitting collapses) from the ideal value of 54.736°. Curve a demonstrates the small deviation from the ideal magic angle in the $B_{\parallel} = h\nu/g_{\parallel}\beta$ region of the spectrum as $g_{\perp}$ is allowed to vary from 1.70 to 2.30. Curve b shows the simultaneous variation of $\zeta = 54.736°$ in the $B_{\perp}$ region as $g_{\perp}$ is varied over the same range.

entation $\zeta = 0°$, $\eta = 0°$, the calculated splitting was approximately 80 G, and for the orientation $\zeta = 60°$ on $\eta = 0°$, the calculated splitting was approximately 110 G. The figure for the variation in the splitting vs. orientation in the g_{yy} region can be gotten by reflecting the surface for the variation in the g_{xx} splitting vs. orientation through a plane that is parallel to the vertical axis and that passes through the points $\zeta = 0°$, $\eta = 0°$ and $\zeta = 90°$, $\eta = 90°$.

Figure 2 (included primarily for the sake of clarity) shows the results expected from the use of eq 1. However, in Figure 3 the variation of ζ_m vs. η_m (the magic angle pair) is quite different and shows the effect of the quantization axis being fixed. In Figure 3, $\zeta_m = 90° - 54.736°$ when $\eta_m = 0°$, and $\eta_m = 54.736°$ only when $\zeta_m = 90°$. These figures clearly demonstrate that, in the general case, there is no unique "magic angle". Using the fact that the dipolar interaction varies as $1/R^3$, one can determine from this set of figures the splittings expected for other separations of the two dipoles.

The effects of **g** tensor anisotropy are shown in Figure 4. Here, the deviations from the ideal magic angle of two identical axially symmetric spin systems are shown ($g_{\parallel} = 2.00$ and $g_{\perp} = 1.70–2.30$; the interspin vector is coincident with the two $g_{\parallel}$ axes). Curve a shows there to be very little deviation from the ideal magic angle in the $g_{\parallel}$ region of the spectrum. Curve b, however, shows a small but significant variation in the magic angle in the $g_{\perp}$ region of the spectrum.

We also examined the case of an axially symmetric spin system ($g_{\perp} = 1.70–2.30$, $g_{\parallel} = 2.00$) interacting with an isotropic ($g = 2.00$) spin system. Both the axially symmetric and the isotropic spin showed very little deviation from the ideal magic angle. The deviations were much like those seen for the $g_{\parallel}$ line of Figure 4.

The other study concerned a comparison between the dipolar splittings that result from a single crystal calculation, and similar splittings deduced by examination of the splittings observed in numerically synthesized powder spectra. The example used was the interaction between two identical rhombic **g** tensors with parallel coordinate systems. The principal g values chosen are typical of the ferredoxins, i.e., $g_{xx} = 2.07$, $g_{yy} = 1.94$, and $g_{zz} = 1.88$. After extensive comparison, we concluded that overlapping

TABLE I: Matrix Elements of General Two-Electron Spin–Spin Exchange Operator

	$\lvert +^1/_2,+^1/_2\rangle$	$\lvert +^1/_2,-^1/_2\rangle$	$\lvert -^1/_2,+^1/_2\rangle$	$\lvert -^1/_2,-^1/_2\rangle$
$\lvert +,+\rangle$	$+^1/_4 J$ $+^1/_4\Gamma_{zz}$	$^1/_4(D_y + iD_x)$ $+^1/_4(\Gamma_{xz} - i\Gamma_{yz})$	$-^1/_4(D_y + iD_x)$ $+^1/_4(\Gamma_{xz} - i\Gamma_{yz})$	$^1/_4(\Gamma_{xx} - \Gamma_{yy})$ $-^i/_2\Gamma_{xy}$
$\lvert +,-\rangle$	$^1/_4(D_y - iD_x)$ $+^1/_4(\Gamma_{xz} + i\Gamma_{yz})$	$-^1/_4 J$ $-^1/_4\Gamma_{zz}$	$^1/_2 J + ^i/_2 D_z$ $+^1/_4(\Gamma_{xx} + \Gamma_{yy})$	$^1/_4(D_y + iD_x)$ $-^1/_4(\Gamma_{xz} - i\Gamma_{yz})$
$\lvert -,+\rangle$	$-^1/_4(D_y - iD_x)$ $+^1/_4(\Gamma_{xz} + i\Gamma_{yz})$	$^1/_2 J - ^i/_2 D_z$ $+^1/_4(\Gamma_{xx} + \Gamma_{yy})$	$-^1/_4 J - ^1/_4\Gamma_{zz}$	$-^1/_4(D_y + iD_x)$ $-^1/_4(\Gamma_{xz} - i\Gamma_{yz})$
$\lvert -,-\rangle$	$^1/_4(\Gamma_{xx} - \Gamma_{yy})$ $+^i/_2\Gamma_{xy}$	$^1/_4(D_y - iD_x)$ $-^1/_4(\Gamma_{xz} + i\Gamma_{yz})$	$-^1/_4(D_y - iD_x)$ $-^1/_4(\Gamma_{xz} + i\Gamma_{yz})$	$^1/_4 J + ^1/_4\Gamma_{zz}$

effects in the powder spectra seriously distorted the observed dipolar splitting. For example, a plot of apparent dipolar splitting vs. ζ, η as in Figure 2 was considerably distorted (by ca. 10° or more) from the true values, as found by a single crystal calculation. Thus, if dipolar splittings are inferred from a powder spectrum by a simple examination of the peak positions (i.e., there is no exchange coupling), there can be serious differences from the true values.

V. Combined Dipolar Plus Bilinear Exchange Interaction

Due to the different dependence of the superexchange and magnetic dipole–dipole interaction on distance, there is a region of interspin separation in which both interactions are comparable in magnitude. This corresponds to the region of about 8–14 Å. In this region, both exchange and dipolar effects may be simultaneously present in a spectrum, although the dipolar effect may appear to be attenuated due to the magic angle effect. It is quite useful, then, to express the dipole–dipole interaction in the same form as the general exchange interaction.

The two-center bilinear spin–spin exchange interaction has the general form

$$\hat{\mathcal{H}}_{ex} = \sum_{i,j} J_{ij}^{EX}\hat{S}_{1i}\hat{S}_{2j} \qquad (7)$$

where $J_{ij}^{EX} \neq J_{ji}^{EX}$ due to the Hermetian and time-reversal symmetry properties of $\mathcal{H}_{ex}$. Now, while this equation has the same general form as eq 6, the dependence of the components of the exchange matrix on the distance and orientation variables R_{12}, ζ, η, α, β, and γ is quite different than for the dipole–dipole interaction. The experimental nature of $\hat{\mathcal{H}}_{ex}$ is expressed by resolving it into scalar, vector, and tensor operator components

$$\hat{\mathcal{H}}_{ex} = J_0^{EX}\vec{S}_1\cdot\vec{S}_2 + \vec{D}^{EX}\cdot\vec{S}_1 \times \vec{S}_2 + \vec{S}_1\cdot\Gamma^{EX}\cdot\vec{S}_2 \qquad (8)$$

Now, let us express both types of spin–spin coupling in terms of a single Hamiltonian operator, by writing the general spin–spin interaction in the form

$$\mathcal{H}_{S_1S_2} = J_0\vec{S}_1\cdot\vec{S}_2 + \vec{D}\cdot\vec{S}_1 \times \vec{S}_2 + \vec{S}_1\cdot\Gamma\cdot\vec{S}_2 \qquad (9)$$

where J_0, $\vec{D}$, and Γ are composed of the individual dipolar and exchange components, as follows:

$$J_0 = J_0^{EX} + J_0^{DD} \qquad (10a)$$

$$D_i = D_i^{EX} + D_i^{DD} \qquad (10b)$$

$$\Gamma_{ij} = \Gamma_{ij}^{EX} + \Gamma_{ij}^{DD} \qquad (10c)$$

and where

$$J_0^{EX,DD} = ^1/_3 \operatorname{Tr} \{J_{ij}^{EX,DD}\} \qquad (11a)$$

$$D_i^{EX,DD} = ^1/_2\{J_{jk}^{EX,DD} - J_{kj}^{EX,DD}\} \qquad (11b)$$

$$\Gamma_{ij}^{EX,DD} = ^1/_2\{J_{ij}^{EX,DD} + J_{ji}^{EX,DD}\} \qquad (11c)$$

This form for the spin–spin coupling coefficients is useful for expressing chemical information about the nature of superexchange (i.e., the scalar component is often the largest), and it is convenient for the use of calculated dipolar coefficients, such as given in Appendix I.

A four by four matrix (corresponding to the spin–spin interaction between two spin 1/2 molecules) of the operator of eq 9 is given in Table I. Equations 10 and 11, and the dipole–dipole coefficients of the Appendix, may be used to obtain the complete spin–spin coupling matrix of $\mathcal{H}_{S_1S_2}$. This matrix is used in the line shape calculations of section VI.

It is instructive to take account of the number of known and unknown quantities involved in these equations, particularly for a minimal number of electronic spins. The general spin Hamiltonian for two interacting $S = ^1/_2$ molecules (omitting biquadratic operators) is

$$\mathcal{H} = \beta\vec{B}\cdot g_1\cdot\vec{S}_1 + \beta\vec{B}\cdot g_2\cdot\vec{S}_2 + \mathcal{H}_{S_1S_2} \qquad (12)$$

This equation contains 21 unknown coefficients: 6 for each **g** tensor (assumed symmetric), and 9 for the general spin–spin bilinear coupling. The information available from experiment is less than this: for a 4-state system, only $3 + 2 + 1 = 6$ different transitions are possible, which may be measured in only three linearly independent (x, y, z) directions. So the 21 unknown quantities can only be matched with 18 possible, independent measurements. If, however, one of the **g** tensors can be independently determined (i.e., from symmetry, or from theoretical considerations), then the entire spin–spin matrix of coefficients can be determined from experiment.

Now, suppose that the nine spin–spin coefficients have all been determined (along with the **g** tensors and their respective Eulerian angles, as well). Then, a unique resolution of these nine quantities into dipolar and exchange components, as implied by eq 11 is impossible, since there are nine known, and 18 unknown quantities. A degree of approximate resolution *is* possible, however, if one makes use of additional information, such as information about the theoretical form of the dipole–dipole and exchange operators.

Let us assume that the point dipole form of $\mathcal{H}_{dd}$ is a satisfactory approximation. Then, letting g_1^P = the principal **g** tensor for spin 1, and α_1, β_1, γ_1 = its Eulerian angles (and similarly for spin 2), we can write for $\mathcal{H}_{dd}$ that

$$\mathcal{H}_{dd} = \mathcal{H}_{dd}(g_1^P, g_2^P, \alpha_2 - \alpha_1, \beta_2 - \beta_1, \gamma_2 - \gamma_1, R_{12}, \zeta, \eta) \qquad (13)$$

Thus, the assumption that eq 12 has been completely determined implies that the dipolar interaction is only dependent on three (as yet undetermined) parameters: R_{12}, ζ, and η, the distance and orientation parameters of spin "2" relative to "1". Since only three of the nine spin–spin coefficients from the solution to eq 12 have been assigned, we may assign up to six coefficients to the exchange operator. Letting α_{ex}, β_{ex}, and γ_{ex} be another set

TABLE II: General (Point Dipole) Magnetic Dipole–Dipole Analysis[a]

Orientation: $R_{12} \parallel z$ axis
Scalar D-D Component, $J_0{}^{DD} = 0.00308$

D-D Vector Components

0.0
0.0
0.0

D-D Tensor Components

0.09801	0.0	0.0
0.0	0.09341	0.0
0.0	0.0	-0.19142

Orientation: $R_{12} \parallel (111)$ Direction (Trimagic Orientation)
Scalar D-D Component, $J_0{}^{DD} = 0.00000$

D-D Vector Components

0.00063
-0.00266
0.00205

D-D Tensor Components

0.00000	-0.09878	-0.09760
-0.09878	0.00000	-0.09533
-0.09760	-0.09533	0.00000

[a] g tensors as in section VI; $R_{12} = 8.0$ Å. Units, GHz.

of Eulerian angles defining a coordinate system in which $\mathscr{H}_{ex}$ is diagonal, we may write

$$\mathscr{H}_{ex} = J_0{}^{EX}\vec{S}_1 \cdot \vec{S}_2'' + D_{ex}[3S_{1Z}S_{2Z}'' - \vec{S}_1 \cdot \vec{S}_2''] + E_{ex}[S_{1x}S_{2x}'' - S_{1y}S_{2y}''] \quad (14)$$

The choice of this set of nine determinable spin–spin coefficients is not unique. One might as well choose another set of nine coefficients in a way which includes three arbitrary covalency parameters in the dipolar interaction

$$\mathscr{H}_{dd} = \mathscr{H}_{dd}(R_{12}, \zeta, \eta, C_1, C_2, C_3) \quad (15)$$

while choosing a simpler form for the superexchange interaction

$$\mathscr{H}_{ex} = \mathscr{H}_{ex}(J_0, D_{ex}, E_{ex}) \quad (16)$$

which is equivalent to assuming that the exchange angles α_{ex}, β_{ex}, and γ_{ex} are known.

We draw three main conclusions from this analysis: (1) a component analysis, deriving separate information, from experiment, about both the dipole–dipole and exchange interactions is possible; (2) a considerable amount of information about both the dipolar and exchange operators can be obtained, in addition to the value of the isotropic exchange coupling coefficient and the dipolar magnetic geometry. Information about the exchange anisotropy, the exchange "orientation", or some dipolar covalency correction terms is also obtainable; (3) the component analysis cannot be proved to be unique, due basically to the fact that the spin–spin coupling coefficients are fundamentally underdetermined. Such analyses may have practical value, however, since conditions exist under which the vector and tensor components of the two-center exchange interaction are limited in absolute value. Such conditions have been stated for the two-center vector coupling (Dzaloshinski–Moriya, antisymmetric anisotropic exchange),[10] and general guidelines to the symmetric anisotropic exchange have been given by Moriya,[11] Bleaney and Bowers,[12] and Smith and Owen.[13]

The component analysis of eq 11 was used in the numerical analysis of the general dipole–dipole interaction used in the line shape calculations of the next section. Table II gives the results for two special cases: orientation R_{12} parallel to the z axis, and R_{12} parallel to the trimagic

orientation. In the first case, the scalar component $J_0{}^{DD} \neq 0$, the vector components vanish (general for $\alpha = \beta = \gamma = 0$), and the tensor components are diagonal. For the latter case, $J_0{}^{DD} = 0$ (general as long as $\alpha = \beta = \gamma = 0$), the vector components are nonzero, and the tensor components are strictly off-diagonal. Thus, for an arbitrary orientation of both molecules with respect to the reference coordinate system, all components of the scalar + vector + tensor operators are generally nonzero.

Another interesting conclusion of the combined spin–spin interactions concerns the correct procedure for dipolar distance estimation in the presence of an isotropic exchange interaction. In this case, the dipolar splitting observed in a spectrum is of purely geometric origin which depends on at least the three variables R_{12}, ζ, and η. Perturbation theory expressions are commonly used for such estimates, which usually contain implicit assumptions about the values of ζ and η. The value of R_{12}, in that case, is arbitrary, being determined as much by the experimental value of the dipolar splitting as by the assumed fixed values ζ_0 and η_0. It follows that, if there is nonzero g value anisotropy, a dipolar distance determination is only correct when R_{12} *and* the spherical angles ζ, η are all three determined: a single determination of R_{12} is not unique, and very likely incorrect. (The neglect of the spherical angles ζ, η in the presence of g value anisotropy is an approximation which frequently appears to lead to incorrect values of R_{12}, i.e., the "incorrect use" cited in section I.)

VI. The Mo(V)–Iron/Sulfur Long-Range Spin–Spin Interaction in Xanthine Oxidase and Xanthine Dehydrogenase

Lowe and Bray have discovered several Mo(V) EPR spectra, observed in experimental preparations containing xanthine oxidase and xanthine dehydrogenase, which they have proved to be due to spin–spin interaction with a distant paramagnetic iron–sulfur group.[9,14] The spectrum discovered first (somewhat more complicated than the one discovered later) is labeled "slow", and is characterized by an isotropic exchange splitting, an isotropic hyperfine splitting due to a nearby proton, and a vanishingly small dipole–dipole splitting. The more recently discovered spectrum, "resting II", lacks the proton hyperfine splitting, but is otherwise similar to the "slow" signal in character. The special feature of both of these spectra is the smallness of the isotropic exchange splitting (comparable in magnitude to the proton hyperfine splitting) and the fact that the dipolar splitting is only barely detectable in the turning points of the (glass-type) spectrum.

The unusual feature of the spin–spin interaction is their conclusion that the Fe/S center and the Mo(V) center are at least 10 Å and possibly as far as 25 Å apart, and that the spin–spin interaction is primarily of superexchange nature. The lower range of values of R_{12} follows from the observation that the Mo(V)···Fe/S "group" must have some structural flexibility (i.e., an accessible range of values of the angles ζ, η), since the EPR signals change in response to the effects of various protein denaturation effects. If the distance between the two centers is anywhere near the upper estimate of 25 Å, then the mechanism of propagation of spin-coupling information between the Fe/S and Mo(V) centers is indeed of great interest. As we will show later, an exchange interaction of the observed magnitude (0.001 cm⁻¹) at a distance of 25 Å would be uniquely different from all previous experimental superexchange experience.

In order to better analyze the combined superexchange and dipole–dipole coupling effects, the spectrum of the slow signal was simulated as a single crystal spectrum. An appropriate spin Hamiltonian was chosen as follows: let
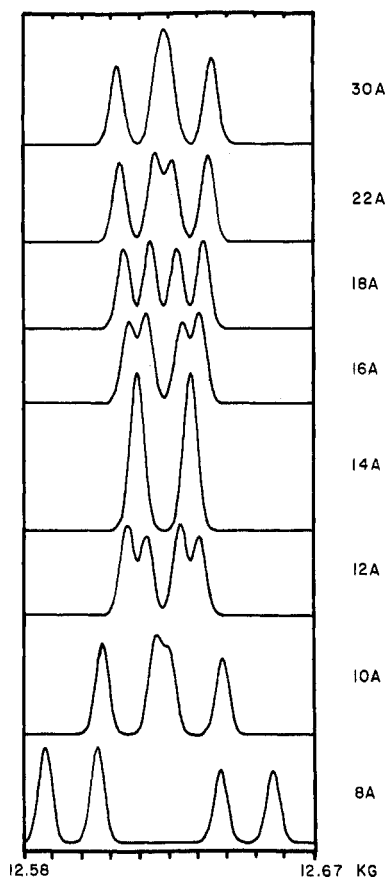
Figure 5. The spectrum calculated for the interaction of an $S_1 = {}^1/_2$, $I_1 = {}^1/_2$ molecule with another having $S_2 = {}^1/_2$ and no nuclear spin. The spin Hamiltonian used is $\mathcal{H} = \beta B \cdot g_1 \cdot S_1 + \beta B \cdot g_2 S_2 + A S_1 \cdot I_1 + J_0 S_1 \cdot S_2 + \mathcal{H}_{dd}$. The **g** tensors are as given in the text with the values of the Eulerian angles set to $\alpha = \beta = \gamma = 0°$. The isotropic hyperfine splitting coefficient was given the value $A = 0.0015$ cm^{-1}, the isotropic exchange coefficient $J_0 = 0.0013$ cm^{-1}. All anisotropic exchange coefficients were set equal to zero. The line width was chosen equal to 1.0 G, as explained in the text, and the line shape is Gaussian. The interspin vector, R_{12}, is oriented along the z axis ($\zeta = \eta = 0°$), and the magnetic field is in the same direction ($\theta = \varphi = 0°$). The dipolar distance R_{12} was allowed to vary from 30 to 8 Å in steps of 2 Å. The reader of this and the following two figures should note the long-range nature of the dipolar splitting, the distance at which dipolar anisotropy is just detectable, and the orientation dependence (both on magnetic field direction and the orientation angles ζ, η) of the splitting. The assumption that J_0 is constant is, of course, unrealistic, but this is necessary to separate the effects of the dipolar splitting from that of exchange. Frequency 34.56 GHz.

$S_1 = {}^1/_2$ for the iron sulfur group, and $S_2 = {}^1/_2$, $I_2 = {}^1/_2$ for the Mo(V) group with a neighboring proton. The spin Hamiltonian then is

$$\mathcal{H} = \beta \vec{B} \cdot \mathbf{g}_1 \cdot \vec{S}_1 + \beta \vec{B} \cdot \mathbf{g}_2 \cdot \vec{S}_2 + \vec{S}_2 \cdot A \cdot \vec{I}_2 + \mathcal{H}_{S_1 S_2} \quad (17)$$

An 8 × 8 complex energy matrix was constructed from this spin Hamiltonian, using two 4 × 4 spin–spin matrices, given in Table I, plus the appropriate Zeeman matrix elements. The 4 × 4 matrix blocks are coupled by the matrix elements of an isotropic $A S_2 \cdot I_2$ hyperfine coupling operator. An EPR rigid lattice absorption line shape was constructed from this matrix, and from the auxiliary radiation matrix, by calculation of the quantity

$$S(\nu_0, B) = \sum_{i<j} P_{ij}(\nu_0, B) g[\nu_0 - \nu_{ij}(B, \Omega)] \quad (18)$$

The methods used for this calculation were the same as described earlier.[1,15] The necessary g values were taken from the literature, i.e., $g_{xx}^{(1)} = 1.972$, $g_{yy}^{(1)} = 1.967$, and $g_{zz}^{(1)} = 1.956$ for the Mo(V) signal,[16] and $g_{xx}^{(2)} = 2.022$, $g_{yy}^{(2)}$
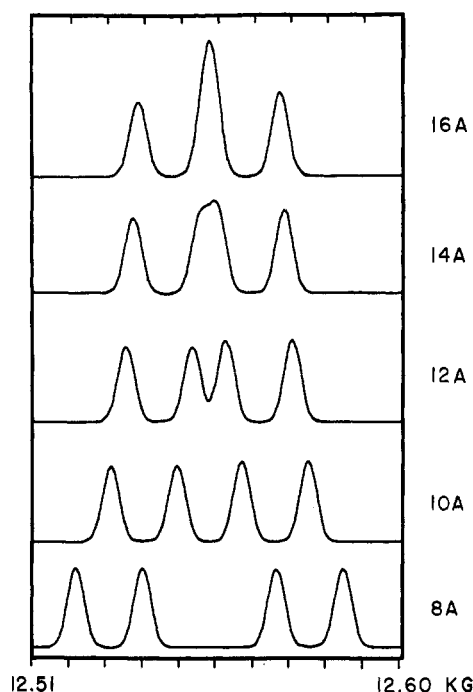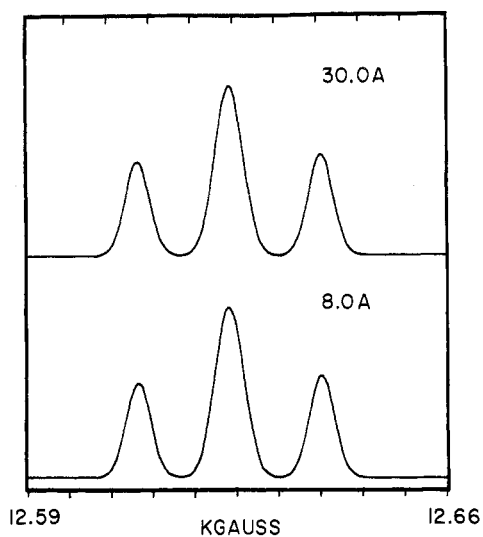
Figure 6. Spin Hamiltonian, g tensors, hyperfine parameter, and line width the same as in Figure 5. The interspin orientation R is also the same, but the magnetic field is parallel to the y axis ($\theta = \varphi = 90°$). Frequency 34.56 GHz.

$= 1.935$, and $g_{zz}^{(2)} = 1.899$ for the Fe/S signal.[17] The two **g** tensors were assumed to be similarly oriented, so that $\alpha = \beta = \gamma = 0°$. The exchange coupling and hyperfine splitting were both assumed to be of scalar form. Both scalar coefficients were assumed to be accidentally equal (as shown by experiment), with the value $+0.0013$ cm^{-1}. A Gaussian type spin-packet line shape was used, with peak-to-peak derivative line width $= 4$ G. A total of ten diagonalizations were made in each sweep interval, using linear interpolation of the selection rule intensities and transition frequencies to fill in the intervening points between diagonalizations. The resulting line shapes were plotted with a high-speed digital plotter.

The spectrum, for the chosen set of parameters, presents a 1–2–1 intensity pattern when the two spin systems are far apart. As the distance parameter R_{12} decreases, the central line initially splits (see Figures 5 and 6), and a more complex pattern develops for smaller distances. The "initial" dipolar splitting was studied vs. R_{12} for two types of geometries: R_{12} parallel to a principal axis (the z axis) and R_{12} along or disoriented from the trimagic angle direction. The results show clearly a range of values of R_{12} showing no dipolar splitting, with a lower-bound value of R_{12} at which value the dipolar splitting is just detected.

If the magnetic geometry is a principal geometry, i.e., with R_{12} parallel to the z axis (for example), and for the magnetic field oriented along the x or y or z axes, then the lower bounds to R_{12} (for *not* detecting the dipolar splitting) are 14.8, 14.4, and 25 Å, respectively, for the assumed criteria for detecting the dipolar splitting (see Table II). Since no dipolar splitting is resolved in any part of the powder spectrum, it is the greatest lower bound (GLB) of the three turning points (x, y, or z) which is of interest. For the case at hand, the GLB or R_{12} is about 25 Å, as quoted by Lowe and Bray. Since this is an unusually long distance for observation of a superexchange interaction (i.e., $J = 0.001$ cm^{-1} at 25 Å is about 10^{10} times larger than predicted by eq 19 at this value of R_{12}), it is important to investigate other geometries for which the GLB may be more reasonable.

Figure 7. Spin Hamiltonian, **g** tensors, hyperfine parameter, and line width the same as in Figure 5. The interspin orientation is trimagic (ζ = 54.736°, η = 45°) and the magnetic field is oriented along the z axis. A $-1.0°$ misorientation of ζ (to 53.763°) is sufficient to generate a marked splitting of the central line for $R_{12} \leq 8.0$ Å. The splitting is much smaller at 55.736°, however, and becomes measurable at 8.0 Å at about $\zeta - \zeta_m = 3.0°$.

Now, if R_{12} is parallel to the trimagic orientation, then the lower bound to R_{12} is on the order of a bond length (see Figure 7), i.e., 2–3 Å (since for a shorter distance, the dipole–dipole splitting, as we use it, has no meaning). Since for this geometry the dipolar distance may have any value, there is no necessity to assume an unusual path length for the superexchange interaction, but this possibility was rejected by Lowe and Bray on grounds of uniqueness. Since they observe no dipolar splitting (other than a line broadening) over a variety of molecular conformations and chemical changes (and for both the slow and resting II signals), the question is whether there is a reasonable size cone of angles about the trimagic orientation within which the GLB to R_{12} is consistent with some limiting R_{12} dependence of J_0^{EX}. Lowe and Bray's estimate for the width of such a cone is $\pm 1°$ (based on a perturbation theory estimate), but we show in Table III that this is much too conservative. The results given in Table III (calculated with parameters chosen to match the slow signal) show that within a cone of angles of about $\pm 5°$ width about (54.763°, 45°), the GLB of R_{12} is about 14 Å, and within $\pm 10°$ about this direction, the GLB is about 17 Å. These estimates for the greatest lower bound to R_{12} are more reasonable than 25 Å, but this fundamental question remains to be answered: for a given value of R_{12}, how large may be the superexchange isotropic J_0^{EX} coefficient, assuming that the superexchange coefficient may have either of the two possible signs?

We have investigated this question (which we report as a separate paper)[18] by studying all available experimental data for which the sign of J_0 is known, its value has been accurately determined, and reliable data on the distance between centers of unpaired spin density is available. Our findings are that ferromagnetic exchange coupling coefficients are always less than or equal to the corresponding values of antiferromagnetic J_0, for the same value of R_{12}, and that the antiferromagnetic isotropic J_0 is bounded, for given R_{12}, by the function

$$|J_0(R_{12}; \text{AFM})| \leq 1.39 \times 10^7 \exp(-1.80 R_{12}) \text{ cm}^{-1} \qquad (19)$$

where R_{12} is measured in angstrom units. Now, Lowe and Hyde have shown, by means of an ELDOR experiment, that the principal splitting in this spectrum (the slow

TABLE III: Lower-Bound Values of R_{12} for which the Dipolar Splitting is Less Than or Equal to (Absorption Line Width)/3

R_{12} orientation parameters	R_{12} (lower bound), Å		
	$B_0 \parallel x$	$B_0 \parallel y$	$B_0 \parallel z$
trimagic orientation: 54.736°, 45.0°	$l_b{}^a$	$l_b{}^a$	$l_b{}^a$
trimagic + $\delta\zeta$ = $-5.0°$	8.0	8.0	13.8
trimagic + $\delta\zeta$ = $+5.0°$	10.6	10.6	~9
trimagic + $\delta\eta$ = $-5.0°$	12.3	8.0	1_b
trimagic + $\delta\eta$ = $+5.0°$	12.1	8.0	1_b
trimagic + $\delta\zeta$ = $-10.0°$	~9	~9	16.9
trimagic + $\delta\zeta$ = $+10.0°$	13.3	13.2	11.0
trimagic + $\delta\eta$ = $-10.0°$	15.2	10.0	$l_b{}^a$
trimagic + $\delta\eta$ = $+10.0°$	10.2	15.3	$l_b{}^a$
principle orientation: 0.0°, 0.0°	14.8	14.4	27

^{a} The symbol l_b stands for a bond length, i.e., the dipolar splitting vanishes in this case for R_{12} down to about a bond length. Other electronic effects take place for shorter distances.

spectrum) is due to an electronic superexchange effect, with $|J_0| \sim 0.001$ cm^{-1}. Since the interaction is known to be ferromagnetic, the maximum value of R_{12} is inferred from the limit function above as equal to 13 Å or less. This value is generally consistent with our conclusions on the allowable range of fluctuation of the dipolar angles ζ, η due, for example, to denaturation effects of the protein. Thus, our conclusions, drawn from the study of both the dipolar spectrum anisotropy (calculated by line shape simulation, rather than perturbation theory) and the "outer-limit" to superexchange property, show that R_{12} probably lies in the range of 8 Å (see Table III) to 14 Å, and that (on the basis of present information) a separation as great as 20–25 Å is ruled out.

VIII. Conclusions

In addition to giving a general description of bilinear spin–spin coupling, we have been able to deduce some apparently useful characteristics of long-range spin–spin coupling effects in EPR. These are as follows. (1) Component analysis of dipole–dipole and exchange coupling coefficients shows that a considerable amount of spin–spin coupling information can be extracted from experiment. (2) It is suggested that there exists an "outer-limit" property of the isotropic exchange coefficient which sets limits to the maximum possible values of antiferromagnetic and ferromagnetic superexchange coupling coefficients at long-range distances. Conversely, a measured value of J_0^{EX} determines an upper bound to the distance between the two centers of unpaired charge distribution (this bound may be smaller for ferromagnetic than antiferromagnetic superexchange, but there is insufficient data at this point to establish the correctness of this assumption). This idea may be useful in the analysis of truly different long-range exchange coupling mechanisms, and it should be equally useful in the analysis of long-range spin–spin coupling effects in macromolecules. (3) Analysis of the magnetic dipolar interaction, in conjunction with the magic-angle effect, shows that this effect becomes increasingly important, relative to superexchange, as the distance parameter R_{12} exceeds about 10 Å, and that for R_{12} greater than or equal to about 15–16 Å (since J_0, according to eq 19, becomes less than the line width of ~ 0.1 G), the dipolar effect only is observable.

These conclusions are particularly significant in relation to the test case which we have found to be most useful, namely, the several types of EPR resonances discovered

by Lowe and Bray in xanthine oxidase and xanthine dehydrogenase systems, which have paramagnetic Mo(V) and iron–sulfur groups which they believe to be separated by distances between 10 and 25 Å. With the aid of qualitative line-shape calculations (see Figures 5 to 7) and our study on long-range superexchange, we are able to further restrict the possible estimates of the distance apart of these paramagnetic groups, without making resort to simulation of the complete spectrum.

More detailed studies on specific model systems and well-characterized macromolecules are necessary in order to determine the usefulness of superexchange properties in relation to, for example, electron transport reactions. It seems possible that experimental and theoretical analysis of spin–spin coupling effects may provide some useful structural and electronic information in inorganic and inorganic biochemistry. It would be particularly helpful, in this regard, to have a better model for the anisotropy of the exchange tensor (Γ_{ij}^{EX}), better than the simple Moriya estimate,[11] which includes the effects of electronic delocalization.

Supplementary Material Available: Derivation of the general expression for the dipole–dipole coefficient $J_{ij}^{DD}(R_{12}, \zeta, \eta, \alpha, \beta, \gamma)$ (2 pages). Ordering information is available on any current masthead page.

References and Notes

(1) G. R. Buettner and R. E. Coffman, *Biochim. Biophys. Acta*, **480**, 495–505 (1977).
(2) G. E. Pake, *J. Chem. Phys.*, **16**, 327 (1948).
(3) J. S. Leigh, Jr., *J. Chem. Phys.*, **52**, 2608 (1970).
(4) C.-C. Chao, *J. Mag. Reson.*, **10**, 1–6 (1973).
(5) S. G. Carr, T. D. Smith, and J. R. Pilbrow, *J. Chem. Soc., Faraday Trans. 1*, **70**, 497–511 (1974).
(6) P. D. W. Boyd, A. D. Toy, T. D. Smith, and J. R. Pilbrow, *J. Chem. Soc., Dalton Trans.*, 1549–1563 (1973).
(7) J. F. Boas, P. R. Hicks, J. R. Pilbrow, and T. D. Smith, *J. Chem. Soc., Faraday Trans. 2*, **74**, 417–431 (1978).
(8) K. L. Schepler, W. R. Dunham, R. H. Sands, J. A. Fee, and R. H. Abeles, *Biochim. Biophys. Acta*, **397**, 510–518 (1975).
(9) D. J. Lowe and R. C. Bray, *Biochem. J.*, **169**, 471–479 (1978).
(10) J. Owen and E. A. Harris, "Pair Spectra and Exchange Interactions" in "Electron Paramagnetic Resonance", Geschwind, Ed., Plenum Press, New York, 1972.
(11) T. Moriya, *Phys. Rev.*, **120**, 91 (1960).
(12) B. Bleaney and K. D. Bowers, *Proc. R. Soc. London, Ser. A*, **214**, 451 (1952).
(13) S. R. P. Smith and J. Owen, *J. Phys. C: Solid State Phys.*, **4**, 1399 (1971).
(14) D. J. Lowe, R. M. Lynden-Bell, and R. C. Bray, *Biochem. J.*, **130**, 239–249 (1972).
(15) R. E. Coffman, *J. Phys. Chem.*, **79**, 1129–1136 (1975).
(16) R. C. Bray, *J. Less-Common Met.*, **36**, 413–417 (1974).
(17) J. F. Gibson and R. C. Bray, *Biochim. Biophys. Acta*, **153**, 721–723 (1968).
(18) R. E. Coffman and G. R. Buettner, *J. Phys. Chem.*, preceding article in this issue.

Analysis of the Concentration Dependence of Nuclear Magnetic Resonance Parameters by Means of Chemical Equilibria. Elucidation of the Complex Formation between Dimethyltin Dichloride and Pyridine Base in Solution

Hideaki Fujiwara,* Fumihiko Sakai, and Yoshio Sasaki

Faculty of Pharmaceutical Sciences, Osaka University, 133-1 Yamadakami, Suita, Osaka, Japan (Received February 5, 1979)

A procedure for the analysis of the concentration dependence of NMR parameters on chemical equilibria, utilizing the Davidon–Fletcher–Powell method of optimization, is described in detail for (1) A + B = AB, (2) A + 2B = AB₂, and (3) A + B = AB (K_1), AB + B = AB₂ (K_2). The procedure is applied to the Me₂SnCl₂ + 2,2'-bipyridine and Me₂SnCl₂ + pyridine systems in CHCl₂CHCl₂, and the coexistence of 1:1 Me₂SnCl₂–pyridine and 1:2 Me₂SnCl₂–pyridine complexes is proven in the latter system. Little has been reported about the former complex. Determination of K_1 and K_2 in the Me₂SnCl₂ + pyridine system is successful by using ^2J(SnH) data (K_1 = 16.6 ± 1.9 dm³ mol⁻¹ and K_2 = 4.44 ± 0.24 dm³ mol⁻¹), when the J of the 1:2 complex is taken as that of the tin compound in a large excess of pyridine, whereas only rough estimates of K_1 and K_2 are available when this J is also regarded as a variable parameter in the calculation. The formation constant of the 1:1 complex in the Me₂SnCl₂ + 2,2'-bipyridine system is 4500 ± 320 dm² mol⁻¹ in CHCl₂CHCl₂, about twice as large as that reported in CH₃CN, and reflects much weaker solvation by CHCl₂CHCl₂ than by CH₃CN.

Introduction

Because NMR spectra of systems containing chemical equilibria reflect an equilibrium average, unless exchange rates are slow enough to allow assignment of peaks to each species involved in the equilibrium, it is necessary to fit the concentration dependence of the data to the NMR parameters of each species. Such an analysis is also valuable in other respects, because it offers quantitative information about the chemical equilibria or intermolecular interactions in solution. In the ordinary NMR measurement, however, it is sometimes difficult to satisfy the familiar condition that the concentration of one component is always much lower than that of the others, which is necessary for several simple graphic methods, such as the Benesi–Hildebrand method. Therefore, in the analysis of concentration dependence of NMR parameters, much